RESILIENT INFRASTRUCTURE
June 1–4, 2016
RESILIENT INFRASTRUCTURE LONDON 2016

INVESTIGATION OF LIVE LOAD MOMENT AND SHEAR FOR THE DESIGN OF BRIDGE DECK SLAB CANTILEVERS WITH UNSTIFFENED EDGE OR BUILT WITH TL-5 BARRIER WALL

Ivan Micovic
Ryerson University, Canada

Dr. Khaled Sennah, Ph.D., P.Eng.
Ryerson University, Canada

ABSTRACT

This study builds on the methods of analyses with respect to cantilever slabs in the Canadian Highway Bridge Design Code (CHBDC), and recommends new simplified equations for the intensity of the transverse moment and shear force at the base of the cantilever overhang due to applied vertical truck loading. A parametric study was conducted using finite-element modelling on bridge deck cantilevers with variable lengths and slab thicknesses. Different end stiffening arrangements were considered, including the presence of PL-3 barriers walls (recently renamed to TL-5) as well as the concrete curb supporting intermittent steel posts carrying the bridge railing. The barrier length changed from 3 to 12 m, while the cantilever length ranged from 1.0 to 3.75 m. The results of this study complement the empirical expressions developed by others to determine the minimum required factored moment and tensile force resistance at the deck-barrier junction, induced by horizontal railing loads. Further to presenting design charts and empirical equations based on a series of cantilever-barrier configurations, this study gives way to the development of a suitable procedure for designing the bridge deck slab.

Keywords: Bridge design, cantilever deck slab, overhang, slab-on-girder, truck load, bridge code, bridge barriers

1. INTRODUCTION

The deck slab cantilever extends in the bridge's transverse direction from the exterior girder, perpendicular to the direction of traffic. While the overhang adds aesthetical value, it also proves to be an economical solution, namely due to reducing the number of girders required. The cantilever overhang is typically designed to vary in height, with its cross-section tapering to a smaller thickness at its free end. Extensive research has been conducted over the years to analyze cantilever slabs in simplified form without an appreciable loss in accuracy. Bakht and Holland (1976) presented a simplified expression for the transverse moment per unit length for unstiffened cantilever slabs of infinite length:

$$[1] \quad M_y = \frac{PA'}{\pi} \frac{1}{\cosh\left(\frac{A'x}{c-y}\right)}$$

The equation allows for the engineer to determine the transverse negative moment at any reference point x and y due to a concentrated load P (Mufti et al., 1993). Graphical charts were also presented for the value of A' for different load-reference points, of various cantilever slabs of varying thickness having ratios of t_2/t_1 of 1.0, 2.0, and 3.0. Jaegar and Bakht (1990) suggested the hyperbolic function in algebraic form:

$$[2] \quad M_y = \frac{2PB}{\pi} \frac{(c-y)^4}{[(c-y)^2 + (Bx)^2]^2}$$

where B is equal to A'/2. Neither equation proves advantageous over the other, and expressions valid only when y is smaller than c (Mufti et al., 1993). Likewise, the moment per unit length is determined for semi-infinite cantilever slabs, valid only in the vicinity of the transverse free edge with reference points along the root of the cantilever, based on the following expression (Bakht and Jaeger, 1985):

[3] $$M_y = \frac{PA'}{\pi}\left[\frac{1}{\cosh\left(\frac{A'x}{c}\right)} + B'e^{-\frac{K\bar{x}}{a}}\right]$$

Bakht and Jaeger (1985) specified that the effect of a concentrated load over a cantilever deck slab becomes negligible beyond a length of approximately 2a in the longitudinal direction. This is illustrated in Figure 1, where the hatched area 2a is treated as the cantilever portion of semi-infinite length, while the central portions that are secluded from either end are treated as cantilever plates of infinite length. In subsequent studies, this region was denoted as $3S_c$ (Bakht and Mufti, 2015), where S_c is the transverse distance from the longitudinal free edge to the supported edge of slabs. The coefficients B' and A' of Equation 3 are obtained from graphical design charts, for different ratios of t_2 / t_1, based on the location of the reference point x or y divided by the cantilever length a. Unlike Equation 2, the equation is valid for reference points only along the root of the cantilever. K is obtained from the following expression (Bakht and Jaeger, 1985):

[4] $$K = \frac{a}{c}\frac{A'B'}{2}\frac{1}{\tan^{-1} e^{-Ax^x/c}}$$

A' and B' are obtained from graphical design charts that are based on the ratio of c/a and the linearly-varying thickness of the deck, but also with the consideration of the ratio of the second moment of area of the slab and edge beam (i.e. I_B/I_S), where I_S can be found from:

[5] $$I_S = \frac{a}{48}(t_2^3 + t_2^2 t_1 + t_2 t_1^2 + t_1^3) = \frac{a}{48}\frac{t_2^4 - t_1^4}{t_2 - t_1}$$

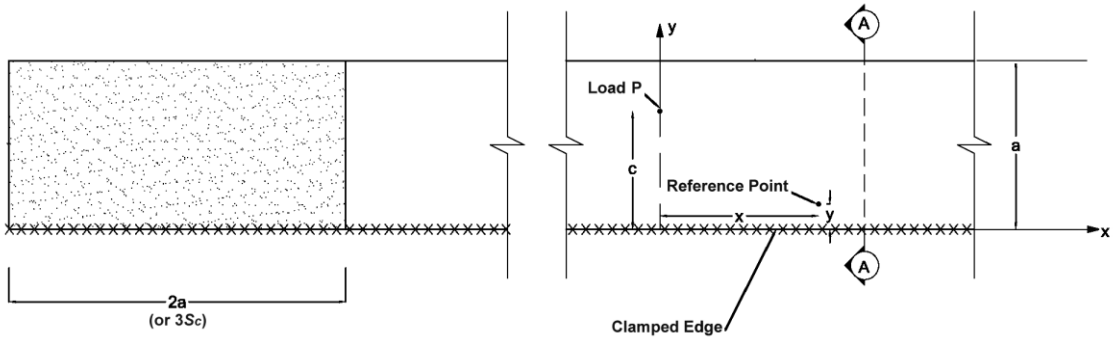

Figure 1: Deck slab cantilever reference points (based on Bakht and Jaeger, 1985)

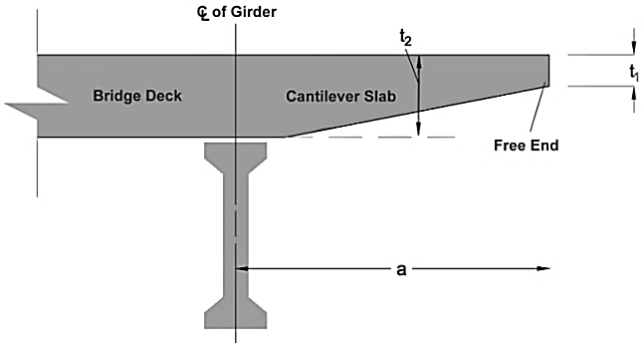

Figure 2: Nomenclature for tapered deck slab cantilever, Section A-A

Mufti et al. (1993) presented a simplified method for analyzing moments in the internal deck slab panels of slab-on-girder bridges, propelled by the fact that the solution proposed by Bakht and Holland (1976) provides the moment intensities solely in the deck slab overhangs. No information is provided for the internal panel adjacent to the overhang. Designers would otherwise have to assume that the peak moment intensity at the root of the cantilever varies linearly into the first panel adjacent to the overhang, per Clause 5.7.1.6.1.2 of the CHBDC (2014):

> *In the absence of a more refined method of analysis, the transverse moments in the interior panel next to the cantilever overhang may be assumed to vary linearly from the values calculated in accordance with Clause 5.7.1.6.1.1 at the root of the cantilever overhang to zero at the girder next to the exterior girder.*

This may lead to an overestimation of the moment in the internal panel and the reinforcement that is required (Mufti et al., 1993). Through their analysis, Mufti et al. (1993) presented that Equation 6 provides the transverse moment intensity in considering the internal panel of the bridge, with the latter equation being its algebraic form:

[6] $$M_y = \frac{2PB}{\pi}\frac{1}{\cosh\left[\frac{2BS_x}{c(S-y)}\right]} \quad \text{and,} \quad M_y = \frac{2PB}{\pi}\frac{c^4(S-y)^4}{[c^2(S-y)^2 + S^2(Bx^2)]^2}$$

When x = 0, the equations above reduce to the following form for maximum moments:

[7] $$M_y = \frac{2PB}{\pi}$$

Tabulated values of B based on different ratios of S/S_c for various values of t_1/t_2 were also presented. An important aspect discovered was that the distribution of hogging moments from the cantilever slab into the internal panel along y was not just nonlinear, but cannot be linear even if the length of the cantilever slab would be large relative to the length of the internal panel. Mufti et al. (1993) demonstrated this for two slabs, denoted as Slab A and Slab B. Slab B was loaded with half the load of Slab A to create the same moment intensity at the root of the cantilever slab, but its distribution into the internal panel proved quite different, necessitating further analysis.

1.1 Canadian Highway Bridge Design Code Provisions

The aforementioned research presently serves as the basis of the section on deck slab moments due to loads on the cantilever overhang in the CHBDC (2014). The intensity of the transverse negative moment M_y at the interior location can be determined as stipulated in Cl. 5.7.1.6.1.1:

[8] $$M_y = \frac{2PA}{\pi}\frac{1}{\left[1 + \left[\frac{A \cdot x}{C-y}\right]^2\right]^2}$$

A replaces A' from previous studies, and is obtained from graphical charts, dependent on whether the cantilever slab is edge-stiffened with a cast-in-place barrier or unstiffened. The exercise of determining M_y at the location of bridge expansion joints, or within a distance of S_p of the transverse free edge, was simplified in the CHBDC (2014) by assuming the design moment in this region as $2M_y$. As an alternative to the equation in Cl. 5.7.1.6.1.1, the maximum transverse negative moment at the root of the cantilever can be determined without calculation from Table 5.10 of the CHBDC (2014).

It is these inferences and conclusions drawn from previous studies, including the assumptions of the CHBDC that necessitated a more rigorous and refined approach that considers the effects of different stiffening arrangements and barrier lengths. The effect of different types of end stiffening arrangements applied onto the slab is important to consider, as it increases the overall flexural rigidity of the section, in turn improving performance and economy by optimizing the amount of reinforcement required. As such, this study is a practical investigation into the different factors that affect the corresponding moment and shear induced in cantilever deck slabs, and examining effects of variables that are presently not considered in the CHBDC.

2. FINITE ELEMENT ANALYSIS

Developed by Computers and Structures Inc., SAP2000 was utilized as part of this study, and in addition to its graphical interface and sophistication, it is able to link to third party applications for user-developed scripts through its Application Programming Interface (API). For the purpose of this study, SAP2000 API enabled the link between Microsoft Excel and SAP2000, using the Visual Basic for Applications (VBA) programming language. This simplified what would have been a more rigorous analysis with multiple cantilever-barrier configurations.

2.1 Material Modeling

The deck slab was considered to be constructed of reinforced concrete, and elastic material properties were used throughout the study. The compressive strength (f'_c) was considered as 30 MPa for all concrete components with a specific weight of 24 kN/m^3. The modulus of elasticity of concrete (E_c) was defined as $4500\sqrt{f'_c}$ and the Poissons's ratio as 0.2.

2.2 Geometric Modeling and Aspect Ratio of Elements

A three-dimensional finite element model with 6 degrees of freedom at each node was generated to simulate each deck slab cantilever. Thin shell elements were selected to model the cast-in-place barriers and deck, with the elements modeled at mid-thickness (centreline) of the deck slab and barrier wall as shown in Figure 3. By utilizing shell elements, the model was simplified to its planar form, reducing the number of equilibrium equations to be solved.

As the centreline approach was utilized for modeling, this is seen as a conservative approach to obtaining results; the moment at the surface would progressively become larger due to the dispersion angle of the load until it eventually reaches the centroid of the section. Given that the deck slab also tapers towards the free end, the thickness was discretized into 5 individual strips to accurately simulate the behaviour of a variable-thickness slab, and this principle is illustrated in Figure 4. The load was applied 300 mm from the curb, and with the actual 600 × 250 mm footprint utilized (87.5 kN or 0.5833 MPa); this meant that the edge of the footprint would be adjacent to the curb. Due to the varying thickness at the base of each stiffening arrangement, the location of the applied live load and its distance from the curb would change accordingly.

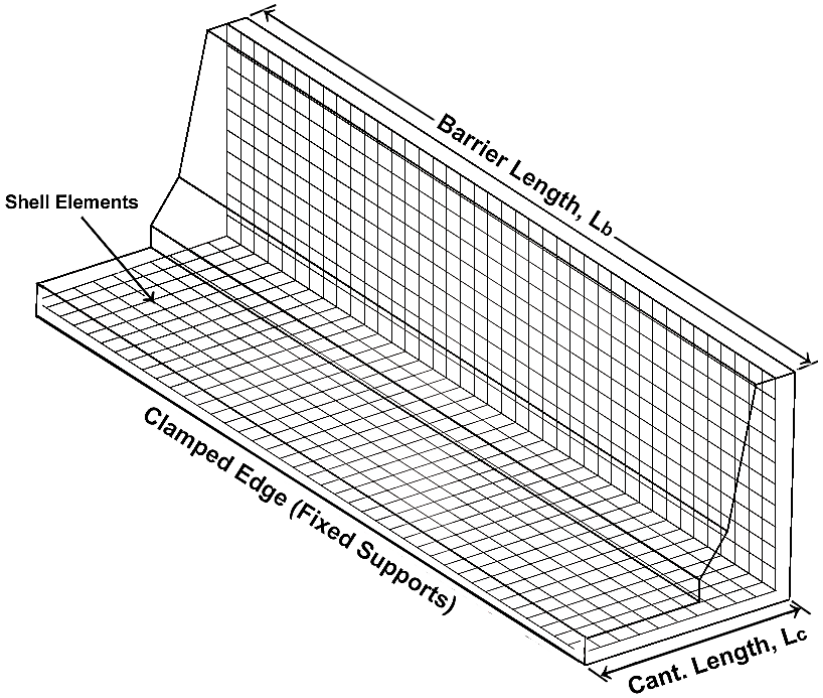

Figure 3: Centreline approach utilized for modeling cantilever slabs

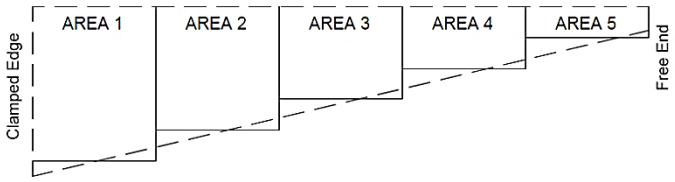

Figure 4: Discretized areas used for modeling cantilever slabs

The thin shell elements were each refined at 50 × 50 mm and were kept at an aspect ratio of 1 for all deck slab elements and barrier wall shell elements, with a maximum of 1.1 appearing in some cases at the barrier wall interface with the cantilever slab. In accordance with the software theory manual (CSI), the refined mesh allowed for a detailed observation of the moment and shear (derived from reactions), thus preserving the accuracy of the data.

3. PARAMETRIC STUDY

The CHBDC (2014) CL-625 design truck was applied to each model and the resulting empirical equations contain the maximum of the largest, single axle of the truck (175 kN) or the effect of two axles (140 kN each). Similar to the current provisions of the CHBDC (2014), upon determining the results, the designer may apply the appropriate load factor from Chapter 3 of the CHBDC (2014) and the corresponding dynamic load allowance stipulated in Table 3.

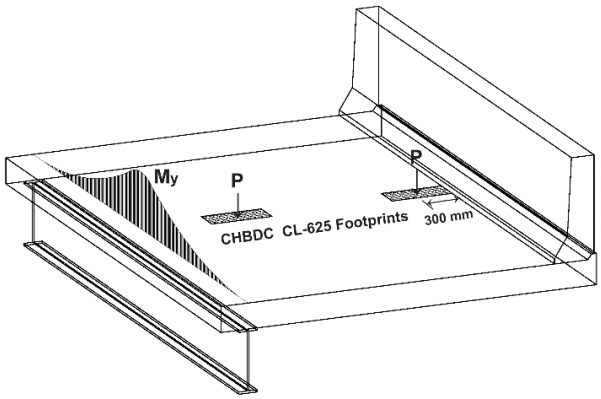

Figure 5: Actual footprints utilized with respect to bridge components (theoretical slab shown)

2.3 Cantilever-Barrier Configurations

A total of 4,284 different SAP2000 models were analyzed to study the transverse moment and shear induced in the bridge cantilever deck slab by the CHBDC truck loading. The following parameters were considered:

1. The type of edge-stiffening applied: Two scenarios most commonly occurring in practice were considered, which included edge-stiffening with PL-3 barriers (presently denoted as TL-5 or Test Level in lieu of PL or Performance Level in the 2014 version of the CHBDC), and an unstiffened edge, representing the case of intermittent steel posts supporting a guiderail.
2. Slab thickness (t_d) and thickness ratio (t_r): Five (5) base slab thicknesses of 200, 225, 250, 300, and 350 mm were considered, including four (4) different thickness ratios for the first 4 thicknesses: t_2/t_1 of 1, 1.2, 1.5, and 2. Parameter t_2 is the thickness at the root of the cantilever, whereas t_1 is at the transverse free end.
3. The length of the cantilever deck slab in the transverse direction: The lengths studied were 1, 1.5, 2, 2.5, 3, and 3.75 m, and the variable is denoted as L_c in this study.
4. The longitudinal slab and barrier length. These values changed from 3, 4.5, 6, 8, 10, and 12 m. It was found that increasing the barrier length beyond a distance of 12 m was asymptotic, and held minimal effect on the transverse moment and shear. The inclusion of the minimum barrier length, considered as 3 m in practice, smooths the data set and was included to complement the studies by others, where barriers of these lengths

were crash-tested at interior and exterior locations. Given the loading was applied at the interior location, the ends of the barrier lengths were characterized the same due to the longitudinal dissipation of moments.

Based on these parameters, a unit length was taken at the maximum location of the clamped edge to determine the transverse moment and shear. For cantilevers stiffened with a New Jersey-shaped barrier, results are compared to Table 5.15 of the 2014 version of the CHBDC, whereas other configurations are compared to Table 5.10 of the previous 2006 version of the CHBDC, since it considers other cast-in-place concrete barrier configurations. The change in longitudinal moment, M_x, was also studied, with a unit length taken at the maximum location near the wheel load, where a more significant sagging moment was observed; however, the data is presented outside of this paper in the report by Micovic (2016).

2.4 Empirical Equations for the Transverse Moment and Shear

The data gave way to the development of empirical equations that may be readily used based on different cantilever-barrier configurations. The coefficients to the equations were determined statistically by the method of least squares; first by means of evolutionary algorithm (a generic population-based metaheuristic optimization algorithm), and subsequently refined through Generalized Reduced Gradient (GRG) nonlinear regression. Coefficients were further adjusted and their number of digits truncated for clarity and simplified use by designers without a loss in accuracy. A constraint was applied such that the resulting moment and shear were not underestimated greater than 5%. Table 1 presents the developed empirical equations for the moment and shear at the interior location for the PL-3 barrier and unstiffened edge, while Figures 6 conveys the validity of the developed equations compared to the results obtained by means of FEA. Additional equations for the PL-1 and PL-2 barriers, PL-2 parapet, and concrete curb, along with additional findings are available in the report by Micovic (2016).

Table 1: Empirical equations for transverse negative moment and shear due to live load*

			PL-3 Barrier	**Unstiffened Edge**
			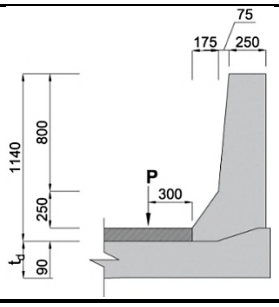	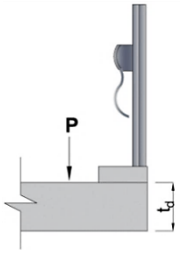
Moment (kN-m/m)	$L_b \leq 6$	$L_c \leq 2.5$	$42L_c^{1.65}L_b^{-1.16}t_1^{-0.72}t_2^{-0.13} + 7$	$24.4L_c^{2.07}L_b^{-0.74}t_1^{-0.28}t_2^{0.28} + 25$
		$L_c > 2.5$	$38L_c^{1.95}L_b^{-0.81}t_1^{-0.034}t_2^{0.1} + 2.5$	$30L_c^{2}L_b^{-0.8}t_1^{-0.14}t_2^{0.14} + 24$
	$L_b > 6$	$L_c \leq 2.5$	$46L_c^{0.88}L_b^{-0.29}t_1^{-0.14}t_2^{0.3} - 3.5$	$25L_cL_b^{-0.09}t_1^{-0.3}t_2^{0.3} + 10$
		$L_c > 2.5$	$53L_c^{1.23}L_b^{-0.34}t_1^{-0.07}t_2^{0.16} - 26$	$63L_c^{0.9}L_b^{-0.17}t_1^{-0.14}t_2^{0.13} - 37$
Shear (kN/m)	$L_b \leq 6$	$L_c \leq 2$	$-378L_c^{-0.12}L_b^{-0.04}t_1^{-0.01}t_2^{0.03} - 277$	$64L_c^{-0.8}L_b^{-0.08}t_1^{-0.2}t_2^{0.2} + 18$
		$L_c > 2$	$104L_c^{0.74}L_b^{-0.36}t_1^{-0.33}t_2^{0..074} - 43$	$2332L_c^{0.017}L_b^{-0.013}t_1^{0.0026}t_2^{-0.0026} - 2222$
	$L_b > 6$	$L_c \leq 2$	$255L_c^{-0.24}L_b^{-0.0096}t_1^{-0.02}t_2^{0.06} - 169$	$72L_c^{-0.65}L_b^{-0.0006}t_1^{-0.17}t_2^{0.17}$
		$L_c > 2$	$31688L_c^{0.0014}L_b^{-0.00034}t_1^{-0.00013}$ $t_2^{0.00033} - 31636$	$32112L_c^{0.001}L_b^{-0.0001}t_1^{-0.0004}$ $t_2^{0.0004} - 32050$

*units are in metres (m)

Table 2: Dynamic Load Allowances for governing loads*

Dynamic Load Allowance, I_D Cl. 3.8.4.5	Transverse Moment due to Live Load		Transverse Shear due to Live Load	
	Single Axle	Tandem	Single Axle	Tandem
	1 + 0.4	1 + 0.3	1 + 0.4	1 + 0.3
Unstiffened Edge PL-3 Barrier	$L_c < 1.5$	$L_c \geq 1.5$	$L_c < 2$	$L_c \geq 2$

*units are in metres (m)

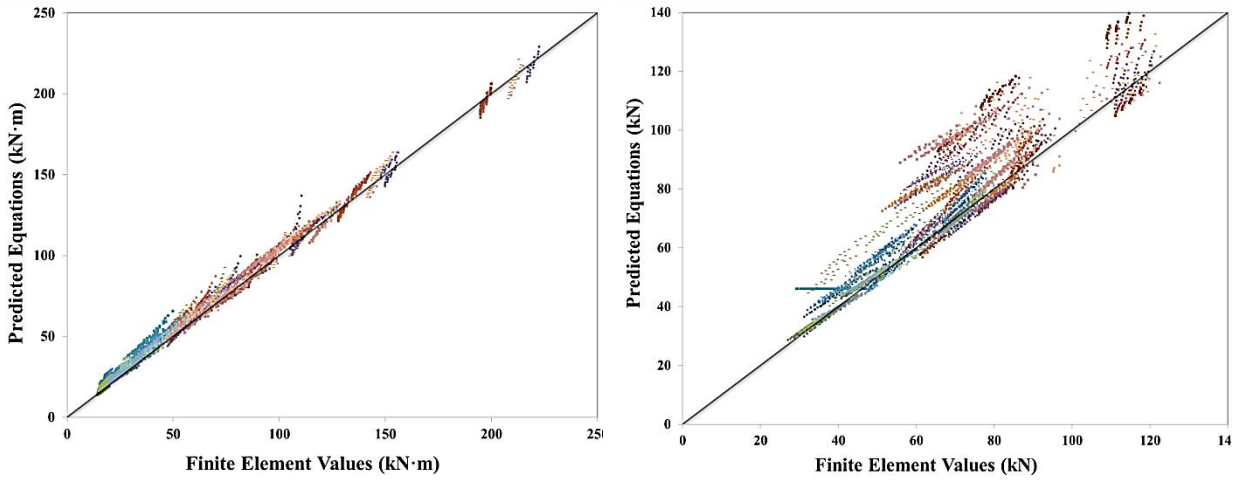

Figure 6: Demonstration of accuracy of developed equations: Predicted equations for transverse negative moment (left) and shear (right) plotted against finite element values for multiple cantilever-barrier configurations

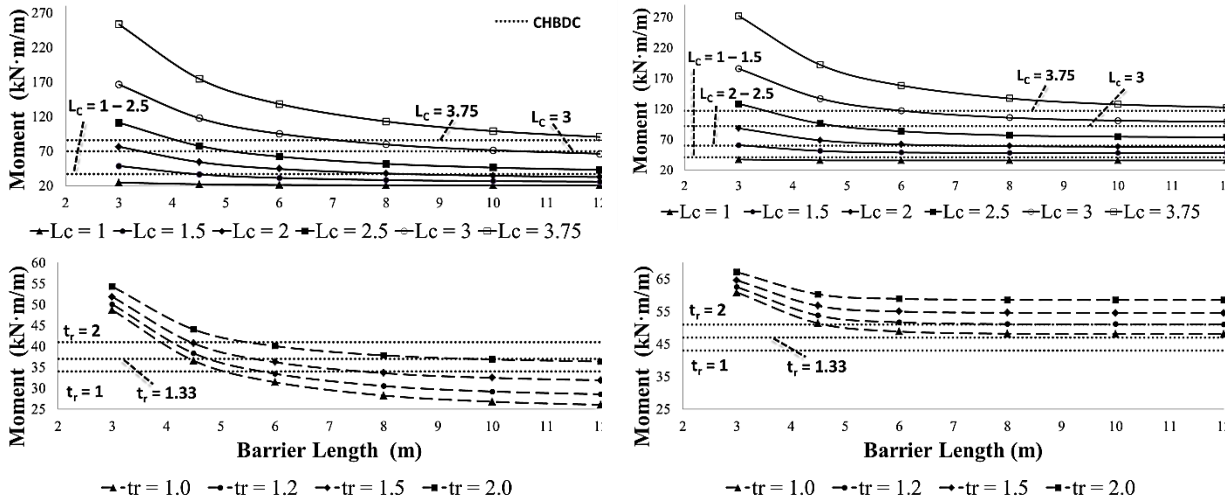

Figure 7: Effect of cantilever length and thickness ratio on moment: PL-3 barrier (left) and unstiffened edge (right)

2.5 Analysis of Results

2.5.1 Transverse Moment

- The effect of stiffening configuration is illustrated in Table 4, where all other parameters are kept constant. It is shown that the addition of the barrier wall decreased the applied transverse negative moment by 41%.
- The barrier length held a great influence on the variation of transverse negative moment. As the barrier length increases, moments that were very large at the clamped edge decrease, and this rate of decrease tends to converge at larger barrier lengths, due to the increased stiffness and load dispersion area.
- The general increase of the cantilever overhang led to the increase in the transverse negative moment. This is an anticipated result due to the increased lever arm, as well as the presence of additional wheel loads with cantilever lengths long enough to accommodate them (e.g. a cantilever length of 2.5 m accommodates a full tandem of 140 kN axles).
- Increasing the slab thickness, and more noticeably the thickness ratio, attributes to the increase in negative moment. It should also be noted that the resisting moment of the section will also increase and in most cases with longer cantilevers, the demand for reinforcement at the clamped edge will decrease.

Table 4: Effect of end stiffening on transverse negative moment

Stiffening Arrangement	Unstiffened Edge	PL-3 Barrier
Moment	40.2 kN·m *	-41%

*Average transverse negative moment for L_b = 12 m, L_c = 1.5 m across all slab thicknesses

2.5.2 Transverse Shear

- It was found that increasing the barrier length beyond 6 m had very little effect on the shear. Generally, increasing the cantilever length would decrease the total induced shear force at the clamped edge due to the increased area available for dispersion; however, this was not the case with all cantilevers, as additional wheel loads may be applied to those with longer lengths to accommodate them.
- The effect of slab thickness was similar to those observed for induced moments. Increasing the slab thickness or thickness ratio attributes to the increase in shear, but also increases the shear capacity of the concrete section. As with previous sections, Table 5 outlines the average increase in shear with each slab thickness ratio.

Table 5: Effect of slab thickness on transverse vertical shear

Thickness Ratio	t_r = 1	t_r = 1.2	t_r = 1.5	t_r = 2
Shear	36.8 kN *	+7%	+15%	+25%

*Average transverse vertical shear for L_b = 12 m, L_c = 1.5 m, t_1 = 225 mm for a PL-2 barrier configuration

2.6 Applicability to Other Design Codes

The developed equations can be modified for other standards accordingly, such as the AASHTO LRFD (2012) methods adhered to in the United States. For scenarios where two 70 kN wheel loads were found to govern over a single 87.5 kN load, this is representative of the design tandem utilized in AASHTO. For instance, the HL-93 design tandem consists of two axles weighing 25 kips (110 kN) at the same spacing as the CL-625 truck's 140 kN axles; 4 ft. or 1.2 m. Results are to be multiplied by a ratio of 110 kN/140 kN or a factor of 0.8. Once converted, the appropriate load factors and dynamic load allowance, denoted I_M in AASHTO LRFD (2012), are then to be applied. Although there is a slight variation in the size of the truck load footprint, a sensitivity analysis conducted separately from this study found that the conversion may be performed without an appreciable loss of accuracy. Likewise, the same approach can be taken to convert the results for other trucks, such as the CL-625-ONT truck used for designing and evaluating bridges in Ontario (CHBDC 2014).

3. CONCLUSIONS AND RECOMMENDATIONS

Results obtained from the FEA of numerous bridge prototypes were utilized to develop empirical expressions for the transverse negative moment and shear at the root of the cantilever as a result of live load. The results would allow for more informed decisions on the actual shear and moment encountered due to live loads, produce a more economical result by saving on reinforcing steel, safeguarding the public, and directly apply results to other codes and standards. The refined, yet simplified equations also take into account parameters that have not yet been considered: the barrier length (L_b), cantilever length (L_c), and different end stiffening arrangements. The type of end stiffening played an instrumental role in resisting moment and shear. In practice, designers use parapets, New Jersey-type barriers, curbs, and other end-stiffening arrangements; however, present code provisions consider only unstiffened cantilevers and those stiffened with a New Jersey-type barrier as part of a simplified approach.

Overall, the CHBDC (2014) tends to underestimate values for M_y and thus the equation for transverse moment should be considered for future revision. The equation in Cl. 5.7.1.3 also heavily relies on graphical design charts, which may result in a loss in accuracy as it is up to the visual interpretations made by the designer. In conjunction with the observations also noted in the parametric study by Xiao (1997), there does not appear to be a benefit to increasing the thickness ratio of the cantilever slab, due to the apparent increase in moment intensity. Nevertheless, the tapered end is beneficial as its increased section provides greater shear and moment capacity at the clamped edge, avoiding a thicker concrete slab in the transverse direction. Based on the results obtained from this practical design-oriented parametric study, the following points of research require further investigations in the future:

1. Study and develop equations for deflection at the interior location, and for the design moment and shear force for stiffened and unstiffened cantilever deck slabs at the location of the transverse free edge and bridge expansion joints.
2. Study and develop equations for deflection due to truck loading conditions in unstiffened and stiffened cantilever deck slabs at the interior location and transverse free edges.
3. Investigate the applicability of the developed equations for PL-3 (TL-5) barriers to other barrier configurations listed in the 2014 version of the CHBDC, including TL-1, TL-2, and TL-4.
4. Investigate the effect of concrete flexural cracking in the response of the studied deck slab cantilevers under truck loading conditions, as well as the equivalent vehicle impact loading to the barrier wall.
5. Investigate the differences in stiffness when overhangs are reinforced with GFRP and determine if the load distributions are comparable.

REFERENCES

Bakht, B. & Holland, D.A. (1976) “A manual method for the elastic analysis of wide cantilever slabs of linearly varying thickness.” Canadian Journal of Civil Engineering, 3(4): 523-530, 10.1139/l76-057.

Bakht, B., & Jaeger, L.G. (1985). Bridge analysis simplified. New York: McGraw-Hill.

Bakht, B., & Mufti, A. A. (2015). Bridges: Analysis, design, structural health monitoring, and rehabilitation. Cham, Switzerland: Springer.

Canadian Standards Association (CSA). (2014). “Canadian highway bridge design code (CHBDC).” CAN/CSA-S6.1-14, Toronto.

Computers and Structures, Inc. (CSI). Integrated structural analysis and design software, SAP2000. Berkley, CA.

Jaeger, L.G. & Bakht, B. (1990). “Rationalization of simplified methods of analyzing cantilever slabs.” Canadian Journal of Civil Engineering, 17(5): 865-867.

Micovic, I. (2016). “Development of empirical equations and tables for the design of bridge cantilever deck slabs under CHBDC truck loading” (Master’s project). Ryerson University.

Mufti, A. A., Bakht, B. and Jaeger, L (1993). “Moments in Deck Slabs due to Cantilever Loads”. Journal of Structural Engineering. dio: 10.1061/(ASCE)0733-9445(1993)119:6(1761).

Xiao, Y. (1997). “Analyses of Reinforced Concrete Cantilever Bridge Decks under the Live Truck Loads” (Doctoral dissertation). Technical University of Nova Scotia.